dipole μ is located, giving rise to a chemical shift $\delta = \Delta H/H$. Ideally this shift can be detected experimentally as a contribution to the chemical shift in the nuclear magnetic resonance (NMR) of a proton located at that position. Paramagnetic and diamagnetic currents give rise to positive and negative chemical shifts of inner protons, respectively. These shifts for protons at arbitrary positions can be obtained either from the ring currents or from the total energy (*3*). Here, we follow the second procedure. The total energy is calculated in the presence of an external magnetic field and of the field generated by a probe-dipole at a given position (*3*). By evaluating the energy difference ΔE between the cases in which the dipole is oriented parallel and antiparallel to the external field, it is possible to extract the chemical shift $\delta = \Delta E/(2\mu H)$.

We have oriented the external magnetic field through the middle of a bond separating two hexagons. We then calculate the ring-current chemical shift along every radial line going through the center of a hexagon or pentagon. In Fig. 2, A and B, we report ring-current chemical shifts for all of the three nonequivalent pentagon directions and the four nonequivalent hexagon directions together with their spherical averages, respectively. Note that the chemical shift at the origin δ_0 is directly related to the ring-current susceptibility χ, $\delta_0 = 2\chi/l^3$ (*2*, *3*), where l is the radius of C_{60}. As can be seen from Fig. 2, the chemical shifts are enhanced by at least an order of magnitude in the vicinity of the surface because of the remarkable ring currents. In the pentagon directions, the external magnetic field is generally deshielded by the ring-currents, whereas it is shielded in the hexagon directions. In Fig. 2, A and B, the largest absolute values are obtained for the cases in which the external field is nearly perpendicular to the plane containing the pentagon or hexagon, respectively. The values in Fig. 2 should be compared to the value of -41.4 parts per million (ppm), which is the ring-current chemical shift obtained at the center of the benzene ring with the external field oriented perpendicular to the plane.

The ring currents in C_{60} are found to be very sensitive to the electronic structure. In fact, a different occupation of the electronic levels completely modifies the current patterns. For instance, in the case of C_{60}^{6-} (that is, the T_{1u} level occupied), all of the currents are found to be diamagnetic and flow around the fullerene. The paramagnetic pentagon ring current is thus peculiar to C_{60}.

Very recently, NMR measurements on fullerenes have been performed that are affected by the presence of ring currents (*11*, *12*). Suzuki *et al.* (*11*) synthesized the dihydrofulleroid H_2C_{61} molecule and measured its proton chemical shifts. In this molecule, the additional carbon atom bridges a bond separating a pentagon and a hexagon. The two inequivalent protons, which are directly above a pentagon and a hexagon, show shifts of 2.87 and 6.35 ppm (*11*). Although the presence of the bridge is expected to modify the local electronic structure (*13*) and thus the ring-current pattern with respect to pure C_{60}, the results in Fig. 2 suggest that the observed difference in the NMR shifts could be related to ring currents in H_2C_{61}.

In another experiment, Diederich and Whetten have measured carbon NMR shifts in C_{60} and higher fullerenes (*12*). In C_{60}, all C atoms are equivalent by symmetry and only one resonance line is observed. In C_{70}, however, there are five inequivalent carbon atoms that give five different NMR lines in a range of 20 ppm. Preliminary calculations for C_{70} show that the ring-current pattern is similar to the one in C_{60}. Again, paramagnetic ring currents are found in the pentagons and diamagnetic ring currents are found to flow around the equatorial region. The latter are stronger in C_{70} than in C_{60}, explaining the diamagnetic susceptibility of C_{70} (*6*). The presence of this complicated pattern of ring currents in C_{70} affects the magnetic fields on the carbon atoms and could be one of the underlying reasons for the spread of observed chemical shifts (*12*).

REFERENCES AND NOTES

1. H. W. Kroto *et al.*, *Nature* **318**, 162 (1985).
2. V. Elser and R. C. Haddon, *ibid.* **325**, 792 (1987).
3. ———, *Phys. Rev. A* **36**, 4579 (1987).
4. P. W. Fowler, P. Lazzaretti, R. Zanasi, *Chem. Phys. Lett.* **165**, 79 (1990).
5. R. C. Haddon and V. Elser, *ibid.* **169**, 362 (1990).
6. R. C. Haddon *et al.*, *Nature* **350**, 46 (1991).
7. R. S. Ruoff *et al.*, *J. Phys. Chem.* **95**, 3457 (1991).
8. T. J. N. Brown *et al.*, *J. Comput. Chem.* **12**, 1118 (1991).
9. F. London, *J. Phys. Rad.* **8**, 397 (1937).
10. R. C. Haddon, *Tetrahedron* **28**, 3613 (1972); *ibid.*, p. 3635.
11. T. Suzuki, Q. Li, K. C. Khemani, F. Wudl, preprint.
12. F. Diederich and R. L. Whetten, *Acc. Chem. Res.* **25**, 119 (1992).
13. R. C. Haddon, *ibid.* **21**, 243 (1988).
14. One of us (A.P.) acknowledges support from the the Swiss National Science Foundation.

29 June 1992; accepted 30 July 1992

Uranium Stabilization of C_{28}: A Tetravalent Fullerene

Ting Guo, M. D. Diener, Yan Chai, M. J. Alford, R. E. Haufler, S. M. McClure, T. Ohno, J. H. Weaver, G. E. Scuseria,* R. E. Smalley*

Laser vaporization experiments with graphite in a supersonic cluster beam apparatus indicate that the smallest fullerene to form in substantial abundance is C_{28}. Although ab initio quantum chemical calculations predict that this cluster will favor a tetrahedral cage structure, it is electronically open shell. Further calculations reveal that C_{28} in this structure should behave as a sort of hollow superatom with an effective valence of 4. This tetravalence should be exhibited toward chemical bonding both on the outside and on the inside of the cage. Thus, stable closed-shell derivatives of C_{28} with large highest occupied molecular orbital–lowest unoccupied molecular orbital gaps should be attainable either by reacting at the four tetrahedral vertices on the outside of the C_{28} cage to make, for example, $C_{28}H_4$, or by trapping a tetravalent atom inside the cage to make endothedral fullerenes such as Ti@C_{28}. An example of this second, inside route to C_{28} stabilization is reported here: the laser and carbon-arc production of U@C_{28}.

Buckminsterfullerene, C_{60}, is the most symmetrical and least chemically reactive member yet discovered of a potentially huge class of closed carbon cage molecules composed of 12 five-membered rings and any number (except 1) of six-membered rings (*1*). The smallest of these, C_{20}, has only one possible structure, the dodecahedron. Each carbon in such a C_{20} cage is bonded to three others with a bond angle of 108°, which is so close to the tetrahedral bond angle of 109.5° that the bare C_{20} molecule would be expected to be extremely reactive, with each carbon striving to passify its fourth "dangling" bond. In fact, despite some theoretical evidence to the contrary (*2*), no indication has ever been found in carbon cluster beams for a particularly abundant bare C_{20} cluster, whereas the fully hydrogenated $C_{20}H_{20}$ molecule, dodecahe-

T. Guo, M. D. Diener, Y. Chai, M. J. Alford, R. E. Haufler, S. M. McClure, G. E. Scuseria, R. E. Smalley, Rice Quantum Institute and Departments of Chemistry and Physics, Rice University, Houston, TX 77251.
T. Ohno and J. H. Weaver, Department of Materials Science and Chemical Engineering, University of Minnesota, Minneapolis, MN 55455.
*To whom correspondence should be addressed.

Downloaded from www.sciencemag.org on February 2, 2010

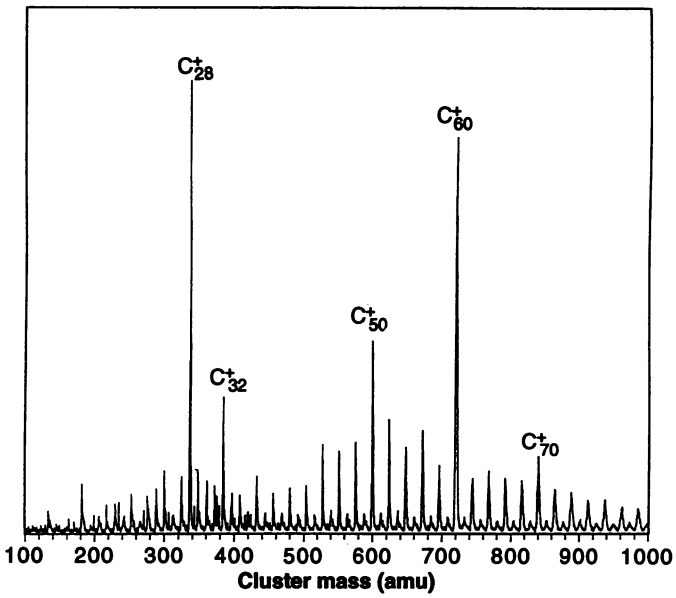

Fig. 1. Time-of-flight mass spectrum of carbon clusters produced in a supersonic beam by laser vaporization of graphite in a pulsed flow of helium. The clusters were ionized by direct 1-photon ionization with an F_2 excimer laser pulse (photon energy, 7.9 eV).

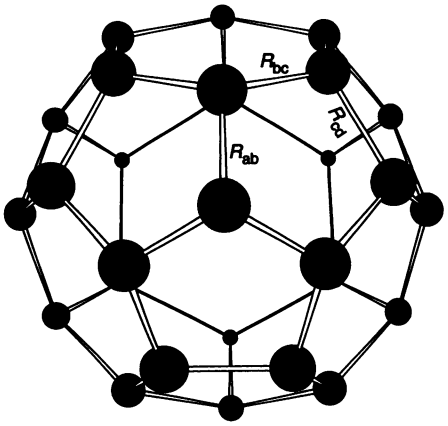

Fig. 2. The T_d symmetry fullerene cage giving the most stable form of C_{28}.

drane, first synthesized by Paquette and co-workers (*3*) in 1976, does turn out to be a highly stable, robust molecule.

With the incorporation of increasing numbers of hexagons, the average bond angle for carbons in the larger fullerene cages increases, tending to the perfect planar sp^2 graphite limit of 120° for cages of infinite size. But, except in the unique case of C_{60} in the perfect I_h symmetry of a soccerball, the strain of curvature necessary to close the carbon network in all larger fullerenes is distributed unequally. It tends to be concentrated at the vertices of the 12 pentagons, and this simple geometrical effect is increasingly pronounced as the cage size increases or whenever two or more pentagons are adjacent. Those carbon positions at which the strain is concentrated will be susceptible to chemical attack. As with $C_{20}H_{20}$, it should be possible to stabilize these more reactive fullerenes by attachment of hydrogen atoms or other monovalent radicals to the most strained sites on the outside surface of the cage.

One particularly attractive possibility is the chemical stabilization of C_{28}. In some of the earliest supersonic carbon cluster beam work carried out at Rice using gentle 1-photon ionization with an F_2 excimer laser to probe the cluster distribution, C_{28} appeared to be the smallest even-numbered cluster that formed with special abundance (*4*). Figure 1 shows a particularly vivid example of such a cluster distribution as produced with a more advanced version of the laser-vaporization cluster beam source (*5*). Here the C_{28} cluster appears to be nearly as special as C_{60} and quite a bit more intense than C_{32}, which is generally the smallest fullerene found in laser "shrink-wrapping" experiments of all larger fullerenes (*1*). Results such as those in Fig. 1 suggest that C_{28} may be the smallest fullerene that forms in abundance in condensing carbon vapors. Modification of the cluster source conditions, thus giving more opportunity for "chemical cooking" of the condensing carbon vapor before expansion, showed that C_{28} does finally react away, leaving C_{60} as the lone survivor, but C_{28} is one of the last such carbon clusters to do so.

Figure 2 shows one possible structure for a C_{28} fullerene (*6*). This structure has been considered briefly in calculations by several groups (*7*). It is the most symmetrical possible structure for 28 atoms: a triplet of pentagons arranged at each vertex of a tetrahedron (symmetry point group: T_d). Direct self-consistent-field (SCF) restricted Hartree Fock (RHF) and analytic energy

Downloaded from www.sciencemag.org on February 2, 2010

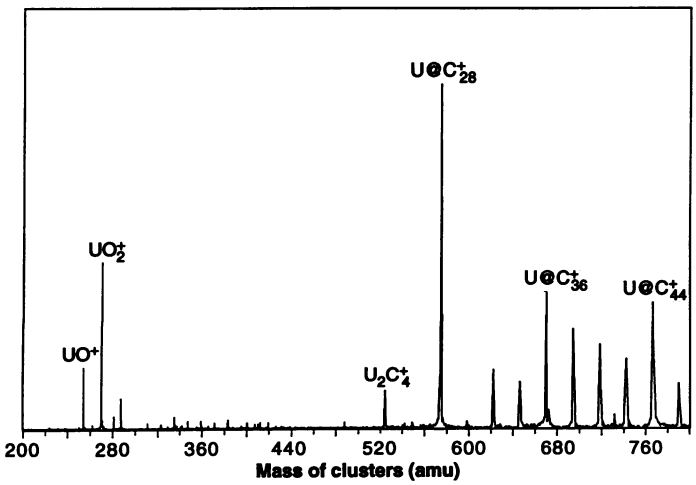

Fig. 3. Fourier transform–ion cyclotron resonance (FT-ICR) mass spectrum of positive carbon-uranium cluster ions produced by laser vaporization of a graphite-UO_2 composite disk, with conditions optimized to view the clusters in the mass range 200 to 500 atomic mass unity (amu). Note that $U@C_{28}$ is the most abundant cluster.

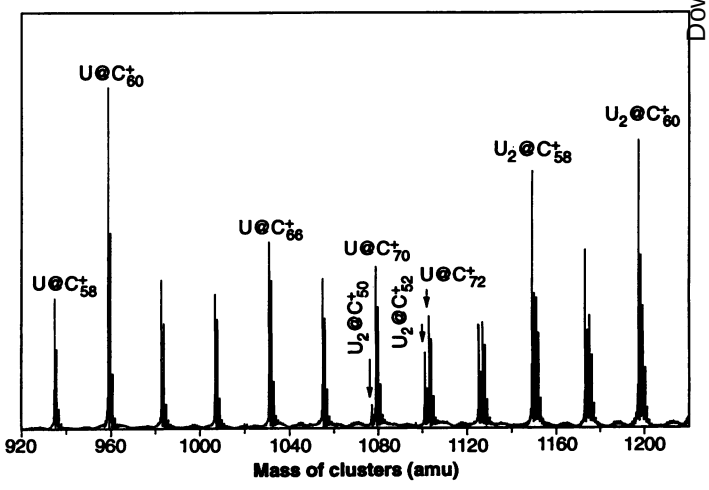

Fig. 4. FT-ICR mass spectrum of carbon-uranium clusters in the larger mass region as produced by laser vaporization of a graphite-UO_2 composite disk. Note the nearly complete absence of empty fullerenes and the dominance of $U@C_{60}$ and $U_2@C_{60}$.

gradient methods (*8*), such as those recently used to study C_{60} (*9*) and tetrahedrally hydrogenated C_{60} (*10*), were applied to C_{28} to obtain the optimized geometry shown in Fig. 2. The ground electronic state of T_d C_{28} was found to be $^5A_2$ with one electron in an a_1 orbital and three in a t_2 orbital, corresponding to a dangling bond located at each of the four carbons at the tetrahedral vertices of the T_d structure. With a double-zeta quality basis set (*11*) the three symmetry-inequivalent equilibrium bond lengths labeled in Fig. 2 as R_{ab}, R_{bc}, and R_{cd} were calculated to be 1.466, 1.400, and 1.539 Å, respectively. The next two excited electronic states of C_{28} in this SCF-RHF calculation $^1A_1$ and $^3T_1$, were found to lie at considerably higher energies (3.2 and 4.1 eV, respectively). The only other possible isomer of C_{28} was found to be a D_2 symmetry structure that lies considerably higher in energy.

The open-shell electronic structure of the $^5A_2$ ground state of C_{28} suggests that addition of four hydrogen atoms at the sites of the dangling bonds would produce a very stable closed-shell molecule, $C_{28}H_4$. Accordingly, an SCF geometry optimization based on the use of a double-zeta basis set was carried out on this molecule. This calculation predicts that $C_{28}H_4$ in T_d symmetry should be an exceedingly stable hydrocarbon with a very large highest occupied molecular orbital–lowest unoccupied molecular orbital (HOMO-LUMO) gap. Upon hydrogenation the calculated bond lengths change to R_{ab} = 1.542 Å, R_{bc} = 1.391 Å, and R_{cd} = 1.528 Å, indicating that this structure is best thought of as four aromatic six-membered rings connected both to each other and to four bridgehead carbons by normal C–C single bonds (*12*).

However, calculations suggest that one may also be able to chemically stabilize C_{28} simply by putting an appropriately sized tetravalent atom on the inside. In fact, we have evidence that this is precisely what has happened in experiments involving production of uranium-doped fullerenes. Figure 3 shows a mass spectral analysis of clusters produced by laser vaporization of a graphite-UO_2 composite target, based on the use of techniques introduced previously to produce La@C_n and Y@C_n metallofullerenes (*13*, *14*). The most abundant species appears to be U@C_{28}. Figure 4 shows the higher mass range of the same mass-spectral analysis. Here it is evident that essentially all the clusters produced are of the form U@C_n. It is clear that a substantial amount of doubly doped fullerenes U_2@C_n, has been made as well, beginning with U_2@C_{50}.

Figure 5 shows the result of a laser "shrinkwrapping" experiment (*1*) on a selected set of U@C_{50}, U@C_{60}, and U@C_{70} clusters. In this experiment, in contrast to any previous experiments with metallofullerenes, the end point of shrinkwrapping is actually below the C_{32} level for an empty fullerene. Thus, the internal uranium atom has apparently stabilized the fullerene cage and made U@C_{28} the end point of laser shrinking.

This evidence that uranium had stabilized the small fullerene cages led us to attempt the bulk synthesis of U@C_{28}, using the methods introduced previously (*13–15*) for other metals. Figure 6 shows the analysis of a sublimed film of fullerenes prepared by laser vaporization of a graphite-UO_2 composite rod in an oven at 1200°C. Similar results were obtained when a dc arc instead of the pulsed laser was used to vaporize this graphite-UO_2 composite rod in the oven. In either case it is clear that U@C_{28} is present in the sublimed film and that it has survived the sublimation process as an intact molecule in the vapor phase at 600°C at least as well as U@C_{60}.

X-ray photoelectron spectroscopy (XPS) was also used to probe the uranium content of these sublimed films. Much as in previous studies with comparable La@C_n and Y@C_n films (*14*), these XPS studies revealed the uranium in this sublimed fullerene film to be in a caged state completely immune to oxidation to form UO_2, even though the film had been exposed to air and water for several days. Comparison of the line shapes and binding energies of the uranium 4*f* core levels measured for U@C_n and UO_2 (*16*, *17*) demonstrated that the uranium in U@C_n was not oxidized. The core level spectra from both U@C_n and UO_2 displayed radically different satellite structures, reflecting substantially different interactions of the core hole with screening orbitals. The main lines of the U@C_n in these films was found to be 1.9 eV lower in binding energy than UO_2, suggesting a more covalent bonding for uranium in the endofullerene form than in the oxide. Indeed, the endofullerene uranium 4*f* binding

Downloaded from www.sciencemag.org on February 2, 2010

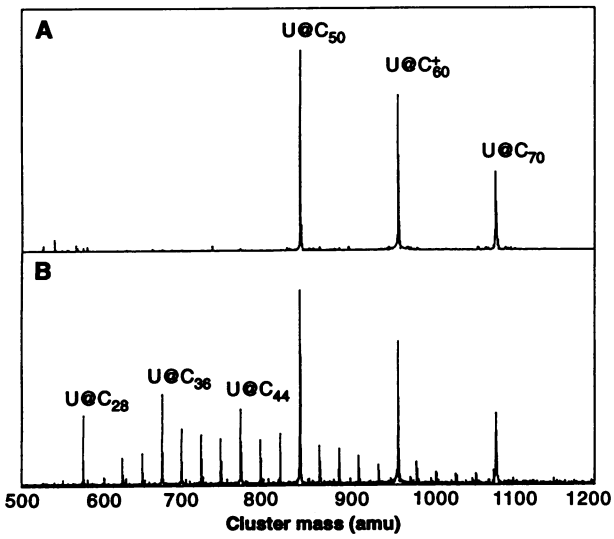

Fig. 5. Laser "shrinkwrapping" experiment on U@C_n uranofullerene ions levitated in the high magnetic field of an FT-ICR analysis cell. (**A**) The initial selection of U@C_{50}, U@C_{60}, and U@C_{70}, clusters. (**B**) The cluster distribution obtained after these selected uranofullerenes were irradiated for 3 s with 150 pulses of a XeCl excimer laser (308 nm) at a fluence of roughly 60 mJ cm^{-2} $pulse^{-1}$ at 50 Hz. The end point of shrinkwrapping the fullerene cage around the central uranium atom is U@C_{28}.

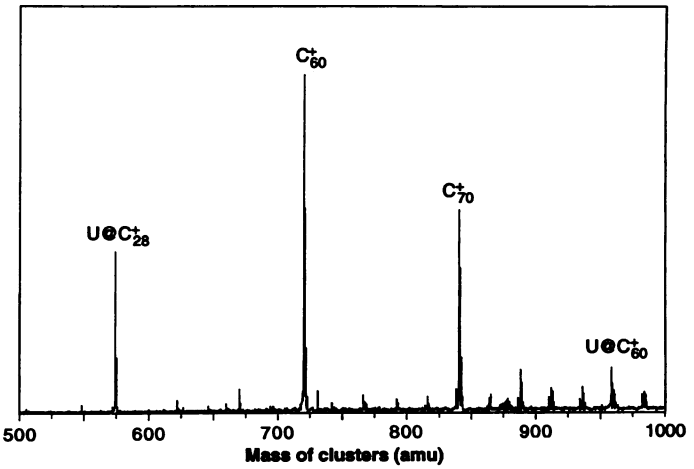

Fig. 6. FT-ICR mass spectral analysis of sublimed film produced from laser vaporization of a graphite-UO_2 composite rod in an oven at 1200°C. Similar results were obtained when the laser vaporization technique was replaced by dc arc vaporization of this same graphite-UO_2 composite rod in the oven. Aside from C_{60} and C_{70}, the dominant cluster species in the sublimed film appears to be U@C_{28}. Moreover, U@C_{60} and higher U@C_n uranofullerenes are present in small amounts. Regardless of the vaporization method used, U@C_{28} and U@C_{60} appear to be produced in good yields, and both appear to sublime as intact molecules along with the empty fullerenes C_{60} and C_{70}.

energy was found to be 377.7 and 388.6 eV for the $j = 7/2$ and 5/2 components, respectively—only 0.5 eV greater than that of uranium metal.

Photoemission spectra for the valence bands of these sublimed films showed strong uranium 5*f* emission, as expected given the high cross section of uranium 5*f* levels relative to carbon states in XPS. The formal valence state can be determined from uranium 5*f* emission centered at a binding energy of ~1.3 eV. The 5*f* signature was consistent with a formal 4+ valence state, in agreement with the assertion that a tetravalent atom has stabilized the fullerene.

The efficiency of formation of $U@C_n$ metallofullerenes evident in these experiments is remarkable. Laser vaporization of freshly prepared graphite-UO_2 composite disks prepared simply by compression of the mixed pure powders were found to routinely produce cluster distributions similar to those of Fig. 4. The relative absence of empty fullerenes shown here suggests that fullerene cages are to some extent actually nucleated in the gas phase around uranium atoms or ions. In our experience, no other element has such a pronounced effect on the fullerene growth. We suspect that this is due to the strong complexing ability of uranium such as it is known to exhibit in uranocene (*18*, *19*) and other similar compounds.

Further experiments showed that the use of a tetravalent internal metal atom to stabilize the C_{28} cage works to some extent with other elements as well. For example, zirconium was found to produce $Zr@C_{28}$ in substantial yield as a result of the laser vaporization of a graphite-ZrO_2 composite target. Similar results have been obtained with hafnium and titanium. The relative abundance of the $M@C_{28}$ cluster of these tetravalently stabilized metallofullerenes was in the order $Ti@C_{28} << Zr@C_{28} < Hf@C_{28} < U@C_{28}$. We suspect that this trend is due primarily to the better spatial overlap of the valence orbitals and the better energetic match of these orbitals for the larger central atom with the valence orbitals of the C_{28} cage. This notion is supported for the first two members of this series by SCF-RHF calculations on $Ti@C_{28}$ and $Zr@C_{28}$, and we expect it will be borne out in future calculations of $Hf@C_{28}$ and $U@C_{28}$ with appropriate relativistic effective core potentials.

The C_{28} fullerene cage therefore appears to have the remarkable property of being tetravalent toward reactions both on the outside and on the inside. Considered as a tetrahedral unit, one can imagine C_{28} interlinked in many ways, including in a simple diamond lattice to form yet another new crystalline form of pure carbon. Our calculations show that the C_{28} unit can exhibit tetrahedral valence on the outside and on the inside simultaneously to form complexes such as $(Ti@C_{28})H_4$. A wide array of new molecules and materials may therefore ultimately be available if these C_{28} fullerene and $M@C_{28}$ metallofullerenes are used as building blocks on a nanometer scale.

REFERENCES AND NOTES

1. R. F. Curl and R. E. Smalley, *Science* **242**, 1017 (1988); *Sci. Am.* **265**, 54 (October 1991).
2. V. Parasuk and J. Almlöf, *Chem. Phys. Lett.* **184**, 187 (1991).
3. L. A. Paquette, R. J. Ternansky, D. W. Balogh, G. J. Kentgen, *J. Am. Chem. Soc.* **105**, 5446 (1983).
4. Q. L. Zhang *et al.*, *J. Phys. Chem.* **90**, 525 (1986).
5. R. E. Haufler *et al.*, *Chem. Phys. Lett.* **179**, 449 (1991).
6. H. W. Kroto, *Nature* **329**, 529 (1987).
7. M. Feyereisen, M. Guotowski, J. Simon, *J. Chem. Phys.* **96**, 2926 (1992), and references therein.
8. R. Ahlrichs, M. Bär, M. Häser, H. Horn, C. Kolmel, *Chem. Phys. Lett.* **162**, 16 (1989).
9. G. E. Scuseria, *ibid.* **176**, 423 (1991).
10. T. Guo and G. E. Scuseria, *ibid.* **191**, 527 (1992).
11. See (*9*) for a detailed discussion of the basis sets and theoretical methods used in these calculations.
12. Efforts to synthesize this highly stable $C_{28}H_4$ hydrofullerene by addition of H_2 or some other hydrogen-bearing species at an appropriate stage in condensing carbon vapors are currently under way.
13. Y. Chai *et al.*, *J. Phys. Chem.* **95**, 7564 (1991).
14. J. H. Weaver *et al.*, *Chem. Phys. Lett.* **190**, 460 (1991).
15. R. D. Johnson *et al.*, *Nature* **355**, 239 (1992); H. Shinohara *et al.*, *ibid.* **357**, 52 (1992); C. S. Yannoni *et al.*, *Science* **256**, 1191 (1992); M. M. Alvarez *et al.*, *J. Phys. Chem.* **95**, 10561 (1991).
16. J. J. Pireaux *et al.*, *Chem. Phys.* **22**, 113 (1977).
17. J. Verbist, J. Riga,, J. J. Pireaux, R. Caudano, *J. Electron Spectrosc. Related Phenom.* **5**, 193 (1974).
18. A. H. H. Chang and R. M. Pitzer, *J. Am. Chem. Soc.* **111**, 2500 (1989).
19. R. M. Pitzer and N. W. Winter, *J. Phys. Chem.* **92**, 3061 (1988).

20. We acknowledge helpful discussions with R. Pitzer and A. Rosen concerning the nature of uranium complexes and uranofullerenes. G.E.S. is a Camille and Henry Dreyfus Teacher-Scholar. This research was supported by the National Science Foundation, the Office of Naval Research, and the Robert A. Welch Foundation and made use of a laser-vaporization cluster beam FT-ICR apparatus supported by the U.S. Department of Energy. Office of Basic Energy Sciences, Division of Chemical Sciences.

5 May 1992; accepted 1 July 1992

Molecular Structure of the Coalescence of Liquid Interfaces

Joel Koplik and Jayanth R. Banavar

When two bodies of liquid merge, their interfaces must also rupture and rearrange into one. Virtually no information is available concerning the small-scale dynamics of this process. Molecular dynamics simulations of coalescence in systems of about 10,000 Lennard-Jones particles have been performed, arranged so as to mimic laboratory experiments on dense liquids. The coalescence event begins when molecules near the boundary of one liquid body thermally fluctuate into the range of attraction of the other, forming a string of mutually attracting molecules. These molecules gradually thicken into a tendril, which continues to thicken as the bodies smoothly combine in a zipper-like merger.

The coalescence of two drops of liquid is, on the whole, a problem of continuum fluid mechanics, but the fine structure of the rupture and the recombination of the drops' interfacial boundaries occur at the scale of molecules. Modeling based on the Navier-Stokes equation successfully captures the evolution of drop shape (*1*–*3*) but lacks a boundary condition or rule derivable from first principles for sewing two interfaces together. Typically, one might say that two interfaces have coalesced when they come within some prescribed (small) distance of each other, and one can then appropriately modify the boundary shape by hand if the subsequent time development is to be calculated. Such an approximation, however, does not allow one to identify cases where drops approach but coalescence does not occur and it also omits a number of potentially significant effects, such as fluctuations in stress as an interface ruptures or the formation of small satellite drops. Furthermore, a complete understanding of coalescence dynamics is invaluable for additional questions such as the entrainment of external fluid or vapor during splashes (*4*) or the disposition of contaminants or surfactants on the drop surface (*5*). More generally, one would like to know more about the microscopic dynamics of the process. We have addressed this question by calculations at the relevant length scale—that of individual molecules.

We consider molecules interacting by the familiar Lennard-Jones interaction (*6*),

$$V_{ij}(r) = 4\epsilon[c_{ij}(r/\sigma)^{-12} - d_{ij}(r/\sigma)^{-6}] \quad (1)$$

J. Koplik, Benjamin Levich Institute and Department of Physics, City College of New York, New York, NY 10031.
J. R. Banavar, Department of Physics and Materials Research Laboratory, Pennsylvania State University, University Park, PA 16802.

Downloaded from www.sciencemag.org on February 25, 2010